Phase relationships between two or more interacting processes from one-dimensional time series. I. Basic theory

N. B. Janson,[1] A. G. Balanov,[1] V. S. Anishchenko,[2] and P. V. E. McClintock[1]
[1]*Department of Physics, Lancaster University, Lancaster, LA1 4YB, United Kingdom*
[2]*Department of Physics, Saratov State University, Astrahanskaya 83, 410026, Saratov, Russia*
(Received 14 March 2001; revised manuscript received 27 July 2001; published 15 February 2002)

A general approach is developed for the detection of phase relationships between two or more different oscillatory processes interacting within a single system, using one-dimensional time series only. It is based on the introduction of angles and radii of return times maps, and on studying the dynamics of the angles. An explicit unique relationship is derived between angles and the conventional phase difference introduced earlier for bivariate data. It is valid under conditions of weak forcing. This correspondence is confirmed numerically for a nonstationary process in a forced Van der Pol system. A model describing the angles' behavior for a dynamical system under weak quasiperiodic forcing with an arbitrary number of independent frequencies is derived.

DOI: 10.1103/PhysRevE.65.036211 PACS number(s): 05.45.Xt, 05.45.Tp, 87.19.Hh

I. INTRODUCTION

To establish from experimental data whether or not two or more interacting processes are synchronized is an old and important problem. In the absence of noise, the existence of synchronization between two processes in interacting limit cycle oscillators was originally taken to imply that their basic frequencies of oscillation are related as integer numbers (i.e., are rationally connected) [1,2], and that their instantaneous phases are permanently locked. This definition suggests that the detection of whether or not synchronization exists can be established by computation of the ratio of basic frequencies in the Fourier spectrum of the signal from one of the subsystems involved. Even in this simplest case, however, the finite observation time and the discreteness of the digitization steps used in practice will make it appear that *all* frequencies are rationally connected, thereby complicating the reliable estimation of their ratio. Furthermore, the noise that is invariably present in all real macroscopic systems means that only effective synchronization [3] can normally take place, meaning that the phases can remain locked only during finite time intervals, and that the basic frequencies may no longer be rationally connected [4]. Serious difficulties may also arise due to the nonstationarity of experimental data.

In view of these problems, modern techniques for establishing the presence or absence of synchronization are based on the assumption that the behavior of each subsystem can be considered separately, and that their individual time series can be compared by a variety of techniques (e.g., by computation of the phase difference between them). This approach has been justified theoretically [3–6] and is widely used to detect synchronization, not only in periodic noisy, but also in chaotic [7–10] oscillators, and even between stochastic [11–15] processes. Its principal assumption is quite reasonable where the system is being forced externally, when one is able to measure both the forcing and response signals [16], or for mutually coupled oscillators of radiotechnical [8,9,17] or biological [18] origin, or for biological systems such as isolated neurons [19], or in any situation when a living system is artificially split into separate subsystems for research purposes, usually by means of surgery or drugs (thereby disrupting its natural functional state) [20–23]. However, in practice there are not many opportunities to measure noninvasively separate signals coming from different interacting processes within a living system: the independent registration of signals derived from respiration and from cardiac activity [24–28] is one of the very rare examples.

It remains an open problem how best to learn from the one-dimensional signal coming from a system, within which several processes with distinguishable time scales interact, whether or not the processes in question are synchronous. In Ref. [29] it was suggested that the interaction of processes in the autonomic regulation of the human cardiovascular system could be studied by the application of ideas from ethnomusicology to univariate time series (heart rate data). However, this approach is tightly linked to the physiological nature of the particular data and cannot be applied in general. Another possibility that has recently been demonstrated [30] is to filter a univariate time series to create two ''separate'' signals that can then be analyzed for synchronization phenomena in the usual ways already developed for bivariate time series.

In the present paper we propose a more general approach towards detecting the presence or absence of synchronization between two or more interacting processes from univariate experimental data. A preliminary report [31] introducing the main idea has already been published. The aims of the present paper are, first, to give an explicit relation between the new variable introduced for univariate data and the conventional variables used in synchronization theory. Second, we extend the approach to encompass the case of several interacting processes.

In Sec. II the basic idea of the approach is outlined, explicit models for the angles of return times maps are derived for an oscillator that is forced either periodically or quasiperiodically, and the relation between the angles and the conventional phase difference is established. In Sec. III the latter relation is demonstrated on a model of nonstationary forced

 ©2002 The American Physical Society

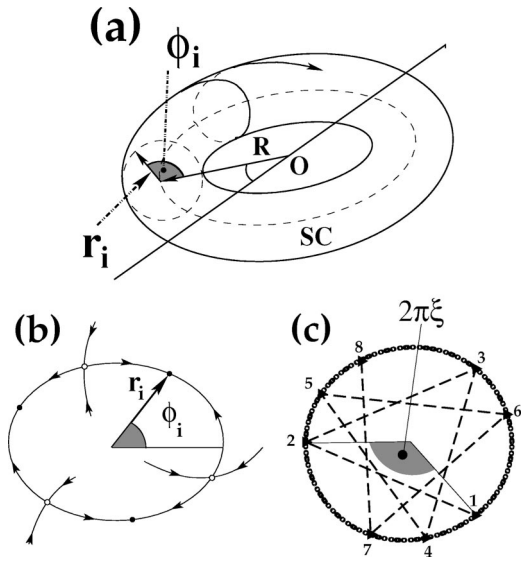

FIG. 1. (a) Surface of a two-dimensional torus. The point *O* is some origin in whose vicinity the motion occurs. The saddle cycle SC (dashed line) is that from which the torus was created as a result of a Hopf bifurcation. The phase trajectory moves along the torus surface and makes two kinds of rotation: around the point *O* with amplitude *R*, and around the cycle SC with amplitude *r*. (b) Poincaré map for a two-dimensional resonant torus inside the region of 1:3 synchronization. Arrows show the direction of stable and unstable manifolds of saddle equilibria. ϕ_i is the current angle, r_i is the current amplitude. (c) Illustration how the points jump on the Poincaré section of a two-dimensional torus.

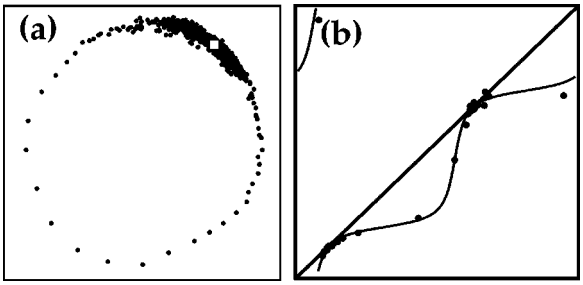

FIG. 2. (a) Stroboscopic section of a Van der Pol system forced periodically and influenced by noise in the region of 1:1 effective synchronization (black points). The white point shows the stable cycle in the noise-free system. Parameter values are given in the text. (b) Map for angles of return times for the case illustrated by (a). The thin black line shows the return function of Eq. (11) for $\xi=1$.

oscillations and the method is tested. The results are summarized and discussed in Sec. IV, and conclusions are drawn in Sec. V.

II. ANALYTIC DESCRIPTION FOR THE IDEAL NOISE-FREE CASE

A. General idea and experimental observations

The central idea of the proposed approach is based on the simple fact that, if *m* periodic processes with different frequencies interact weakly enough within a single system, an *m*-dimensional torus exists in its phase space [2]. The case of two interacting processes is illustrated by Fig. 1(a), showing a two-dimensional torus as the attracting set. To quantify motion on this torus, the *rotation number* ξ is introduced as the ratio between the basic frequencies of the interacting oscillators. It specifies how many periods of one oscillator fall within a single period of the other oscillator.

If the processes are *not synchronous*, the rotation number is irrational. The phase trajectory then fills the whole torus surface and is never closed, and thus its Poincaré map is a closed curve. If the processes are *synchronous*, the rotation number is rational. In this case, distinct stable and unstable cycles lie on the torus surface, and the phase trajectory tends towards the stable limit cycle. The Poincaré map consists of one or several stable points belonging to the stable cycle and an equal number of saddle points belonging to the saddle cycle lying between the stable points on the closed curve formed by the unstable manifolds of the saddles as shown in Fig. 1(b). To consider the dynamics of the Poincaré map, place the origin somewhere inside the region bounded by the closed curve and introduce the phase angle ϕ_i and phase radius r_i [Fig. 1(b)]. At each discrete time moment t_i when the trajectory returns to the Poincaré secant surface, the phase vector rotates by some angle. It is obvious that for the synchronous regime there is a discrete number of possible values of ϕ_i, and for the asynchronous one the angle ϕ_i may take any value between $[-\pi;\ \pi]$. The geometrical meaning of the rotation number is then the average angle by which the phase vector rotates at each step [Fig. 1(c)],

$$\langle \phi_i - \phi_{i-1} \rangle = 2\pi\xi, \tag{1}$$

where $\langle \cdots \rangle$ means an average over time.

If some general noise (with large enough tails in its distribution) perturbs the system, only effective synchronization can take place [3]. In terms of the Poincaré section this means that, at every step, noise prevents the phase point from jumping exactly to the stable point, but makes it jump instead to the vicinity of the stable point. However, at a certain moment, a large enough fluctuation may throw the phase point outside the region bounded by the two stable manifolds of the nearest saddle points, and the phase point then moves along the unstable manifold to another stable point [Fig. 1(b)]. The latter stage of the dynamics is associated with *phase slip*. Thus, instead of one or a few discrete points, one observes one or a few clouds of points smeared around the stable equilibrium/equilibria, and possibly also the trace of the unstable manifolds forming the torus. The latter situation is illustrated by Fig. 2(a) where a stroboscopic section is shown for a Van der Pol system under harmonic forcing while affected by Gaussian white noise,

$$\dot{x}=y;\ \ \dot{y}=\epsilon(1-x^2)y-\omega_0 x+C\sin\Omega t+\sqrt{D}\mu(t). \tag{2}$$

Here, the nonlinearity parameter $\epsilon=0.1$, eigenfrequency $\omega_0=1$, forcing amplitude $C=0.1$, forcing frequency $\Omega=1.025$, $\mu(t)$ is a random value with a Gaussian distribution, zero average and unity variance, and the noise variance $D=0.1$. For these parameter values, effective 1:1 synchroni-

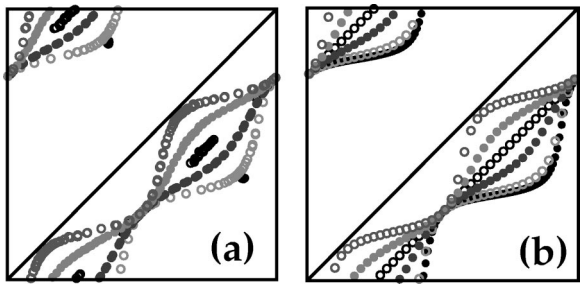

FIG. 3. (a) Map for angles of return times for the Van der Pol system under periodic forcing with fixed small amplitude and different values of rotation number. (b) A series of return functions of map (11) for different values of rotation number ξ close to those in (a). Moving down from the diagonal, the plots sequentially correspond to [according to relation (12)]: $\xi=0.1$ (and 0.9), $\xi=0.2$ (and 0.8), $\xi=0.25$ (and 0.75), $\xi=0.3$ (and 0.7), $\xi=0.4$ (and 0.6), $\xi=0.5$.

zation takes place. In Fig. 2(a) black points show the stroboscopic map of system with noise, and the white diamond in among the bulk of the black ones shows the position of the stable cycle in the noise-free system. Here, the angle ϕ_i can take any possible values, but those corresponding to the vicinity of stable equilibrium are the most probable. Effective synchronization manifests itself in a sharp increase in the duration of the time intervals without phase slips.

According to the Takens theorem [32] and its extension to noise-affected system [33], the system's attractor can be reconstructed from its one-dimensional time series. Obviously, the Poincaré map can also be restored from the reconstructed phase trajectory, being topologically equivalent to that of the original system. In Refs. [34,35] it is shown that the same map can be reconstructed from return times of the system.

Consider a map for the angles of a return times map,

$$\phi_i = f(\phi_{i-1}). \tag{3}$$

The technique of plotting such a map has already been applied to reveal determinism in the *R-R* intervals of anesthetized dogs [36] and in the human heart rate during paced respiration [37], and in jet atomization [38]. The distinctive shape of the maps observed in all these works was attributed to interaction between the particular processes involved. Herzel *et al.* [36] and Suder *et al.* [37] suggested approximate empirical models to describe the dynamics of such maps, but without linking them to the general theory of synchronization or developing an analytic description.

Some typical examples of such a map are shown in Fig. 3(a) for the noise-free Van der Pol system (2) with $\epsilon=0.1$ and the small forcing amplitude $C=0.01$, for several values of forcing frequency Ω varying from 0.25 to 0.9. The basic frequency of the oscillations is close to $\omega_0=1$, and thus the rotation numbers ξ are close to the corresponding values of Ω. Note that, for $\xi=1/2$, one observes a 1:2 synchronization that is reflected by the presence of only two points in the map of Fig. 3(a) (the most distant point from the diagonal in the lower-right part of the picture and the closest point to the diagonal in the upper-left part), and that the whole return function is not seen here since we removed all transients. All the other regimes appear not to fall within the synchronization tongues. Here and in what follows, the axes of the maps for angles have the limits $[-\pi;\ \pi]$.

B. Derivation of the map for angles of return times map for two interacting processes

In this subsection we will clarify the physical meaning of the angles of return times map and will relate it to the conventional phase difference. We will also derive the map describing the evolution of angles with time.

Consider a very simple case of a forced system, namely, a periodic self-sustained oscillator with eigenfrequency ω_0 and amplitude R that is forced harmonically at frequency Ω and amplitude r. As a result of the forcing, a two-dimensional torus is born [Fig. 1(a)]. If the nonlinearity in the oscillator is weak, its autonomous solution can be approximated by a sinusoidal function of time, and the oscillator is then called quasiharmonic. If the harmonic forcing is also weak, $r \ll R$, the solution of the resulting nonautonomous equations can be approximated by a superposition of: one sine term coming from the unforced system and describing rotation around some origin O, i.e., oscillations with frequency ω and amplitude R [as shown in Fig. 1(a)]; and a second sine term corresponding to rotation around the saddle cycle (SC) (the former limit cycle of the autonomous system from which the torus was born via a Hopf bifurcation), i.e., oscillations with the frequency of external forcing Ω and amplitude r. Thus

$$x(t) = R\sin\omega t + r\sin(\Omega t + \phi_0), \quad r \ll R, \tag{4}$$

where ϕ_0 is the initial phase shift. Note that frequency ω coincides with the eigenfrequency ω_0 of the autonomous system in the absence of synchronization. In the presence of synchronization, it is shifted in the direction defined by the forcing. If the oscillations are synchronized by the forcing, the rotation number of the whole system under consideration, here denoted as $\xi=\Omega/\omega$, is equal to n/m, where n, m are integers.

Define the return times of the system as the time intervals between successive crossings by the signal $x(t)$ of a threshold $x=0$ in one direction. To find the time moments t_k of these crossings one should solve the transcendental equation $x(t)=0$, which in general has no analytic solution. Let us make use of the fact that the first term is much larger than the second one, and, therefore, that the times t_k of zero crossing by $x(t)$ are close to the times $t_k^* = \pi k/\omega$ of zero crossing by $(R\sin\omega t)$. We expand the function $x(t)$ as a Taylor series in the vicinity of t_k^*, considering only the linear term and neglecting all the others:

$$x(t) = R\sin\pi k + r\sin\left(\frac{\Omega}{\omega}\pi k + \phi_0\right) + R\omega\left(t - \frac{\pi k}{\omega}\right)\cos\pi k + r\Omega\left(t - \frac{\pi k}{\omega}\right)\cos\left(\frac{\Omega}{\omega}\pi k + \phi_0\right) = 0.$$

Noting that $\cos\pi k = (-1)^k$, and in order to consider every second zero crossing so as to register intersections in only one direction, we set $k=2i$,

$$\left(t-\frac{2\pi i}{\omega}\right)\left[R\omega+r\Omega\cos\left(\frac{2\pi i\Omega}{\omega}+\phi_0\right)\right]=-r\sin\frac{2\pi i\Omega}{\omega}.$$

The t we seek is the ith moment of crossing,

$$t_i=-\frac{r\sin\left(\frac{2\pi i\Omega}{\omega}+\phi_0\right)}{R\omega+r\Omega\cos\left(\frac{2\pi i\Omega}{\omega}+\phi_0\right)}+\frac{2\pi i}{\omega}. \tag{5}$$

Divide the numerator and denominator of the first term of Eq. (5) by r. Since $R\gg r$, and thus in the denominator the first term is much larger than the second one, we neglect the second term and thus obtain

$$t_i\approx-\frac{r}{R\omega}\sin\Psi_i+\frac{2\pi i}{\omega}, \tag{6}$$

where $\Psi_i=(2\pi i\Omega/\omega+\phi_0)$. Denote $\Theta=2\pi\Omega/\omega=2\pi\xi$. Then the expressions for the time moments t_i, t_{i+1}, t_{i+2}, t_{i-1} may be written by analogy. The return times T_i are the differences between the successive times t_i:

$$T_i=t_{i+1}-t_i=-2\frac{r}{R\omega}\cos\left(\Psi_i+\frac{\Theta}{2}\right)\sin\frac{\Theta}{2}+\frac{2\pi}{\omega}.$$

Put the origin into the central point of the return times map (T_i,T_{i+1}) found as an average of all values T_i which is equal to $2\pi/\omega$. Introduce the angle between the current point and the horizontal axis as follows:

$$\phi_i=\arctan\left(\frac{T_{i+1}-\frac{2\pi}{\omega}}{T_i-\frac{2\pi}{\omega}}\right). \tag{7}$$

Then $\tan\phi_i$ is

$$\tan\phi_i=\frac{\cos\left(\Psi_i+\frac{3\Theta}{2}\right)}{\cos\left(\Psi_i+\frac{\Theta}{2}\right)}=\cos\Theta-\tan\left(\Psi_i+\frac{\Theta}{2}\right)\sin\Theta. \tag{8}$$

Similarly, we obtain for $\cot\phi_{i-1}$,

$$\cot\phi_{i-1}=\frac{\cos\left(\Psi_i-\frac{\Theta}{2}\right)}{\cos\left(\Psi_i+\frac{\Theta}{2}\right)}=\cos\Theta+\tan\left(\Psi_i+\frac{\Theta}{2}\right)\sin\Theta.$$

Since

$$\tan\phi_i+\cot\phi_{i-1}=2\cos\Theta, \tag{9}$$

we obtain the following expression for the rotation number ξ:

$$\xi=\frac{1}{2\pi}\arccos\frac{\tan\phi_i+\cot\phi_{i-1}}{2} \tag{10}$$

and an explicit form of the map (3) for angles ϕ_i:

$$\phi_i=\arctan(2\cos2\pi\xi-\cot\phi_{i-1}). \tag{11}$$

Equations (10) and (11) are the final formulas [39] connecting two successive angles of the return times map with the rotation number ξ in the approximation of a quasiharmonic oscillator under weak harmonic forcing. Note that Eq. (11) was quoted earlier as Eq. (6) of Ref. [31], without detailed justification.

C. Analysis of angles for two interacting processes

First, note that, if the amplitude of forcing is much smaller than the amplitude of natural oscillations in the system, the map (3) does not depend on the amplitudes and is completely defined by the rotation number ξ. The ambiguity in defining the value of arctan that is periodic with the period π, not 2π, implies that the return function in Eq. (11) is not continuous but makes a jump by π at the point $\phi=0$, thus being not one-to-one. Moreover, the function arctan itself varies between $-\pi/2$ and $\pi/2$. To draw the return function for angles in a proper way, reflecting its distinct physical meaning, we just leave the value of ϕ_i if $\phi_{i-1}\geqslant0$ and subtract π from ϕ_i if $\phi_{i-1}<0$. When referring to maps (11), or (19) below, we will assume them to have been extended by this procedure.

Second, note that the map (11) does not depend on the initial phase shift ϕ_0 between the solution components.

Third, note that the return function of Eq. (11) is periodic with respect to the variable ξ with period 1, because the cosine function takes equal values for the arguments $2\pi\xi$, or $2\pi\pm2\pi\xi$, or $2\pi l\pm2\pi\xi$ (where l is an integer) if $0\leqslant\xi\leqslant1$. Denote $\xi^*=(1/2\pi)\arccos(\cos2\pi\xi)$, so that ξ^* or $(1-\xi^*)$ is the fractional part of the true rotation number lying within the interval $[0;1]$. Then the true rotation number ξ can be expressed via ξ^* as

$$\xi=\xi^*+l,\quad\text{or}\quad\xi=(1-\xi^*)+l. \tag{12}$$

Thus, from the map for angles only ξ^* can be defined. To select one of the two formulas in Eq. (12) and find l, the Fourier spectrum of the original signal $x(t)$ can be helpful, since for this purpose only a rough estimate of the basic frequencies is required. To simplify further consideration, we will take ξ to mean the value of ξ^* which in all numerical or real data examples given in this paper coincides with true rotation number.

Fourth, it follows from Eq. (11) that (i) if $\xi=1/4$, the return function is the straight line $\phi_i=\phi_{i-1}-\pi/2$ (ii) for any value of ξ the return function passes through the points $(0;-\pi/2)$ and $(\pi;\pi/2)$ and touches the line $\phi_i=\phi_{i-1}-\pi/2$ at these points.

A series of return functions of Eq. (11) for several values of ξ between 0.25 and 0.9 inclusive [the same values as in Fig. 3(a)] are shown in Fig. 3(b). The results are in good agreement with Fig. 3(a), showing that return functions derived theoretically appear to coincide with those obtained from a numerical simulation.

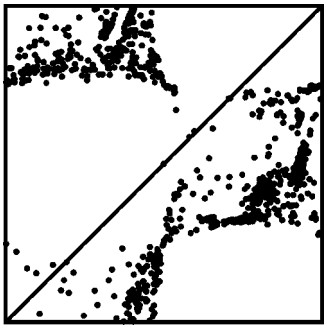

FIG. 4. Map for angles of return times for the periodically forced Rössler system in a chaotic regime. The parameter values are given in the text.

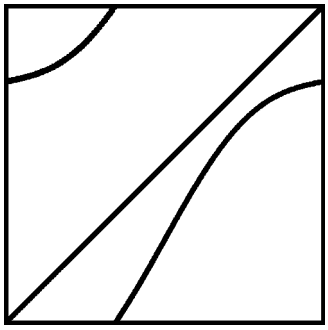

FIG. 5. Return function of a classical sine circle map.

Our numerical simulation has demonstrated that closely similar angles maps appear in the case when two periodic oscillators are coupled mutually and weakly; they are not shown here because they are equivalent to those for the forced Van der Pol system (2) for the same rotation numbers [Fig. 3(a)]. Another useful observation is that even in the case when a weakly chaotic oscillator is forced periodically, the map for angles may sometimes look very similar to that for noise-influenced forced or interacting periodic oscillators. In Fig. 4 a map for angles of return times is given for the Rössler oscillator [40] in a chaotic regime forced periodically. The form of the equations is taken to be as in [41] with the following parameters values: eigenfrequency $\omega=1$; $\alpha=0.2$; $\beta=0.2$; $\mu=10$; and the forcing frequency $\omega_1=0.3$ with amplitude $C=0.5$.

To reveal the physical meaning of the angles, return to Eq. (8). Here, Ψ_i is the phase of external forcing taken at the time moments $2\pi i/\omega$ when the phase of basic oscillations with frequency ω changes by 2π. Note that in general Ψ_i defines the phase of external forcing up to some constant. If Ψ_i is wrapped into the interval $[-\pi;\pi]$ [which does not change the value of $\tan(\Psi_i+\theta/2)$], it is by definition the so-called relative phase introduced in Ref. [25]. Consider the phase difference between two signals, $\tilde{\Psi}(t)=\Phi_1(t)-\Phi_2(t)$, and the values of $\tilde{\Psi}$ at time moments t_i when the phase of one signal, e.g., Φ_2, changes by 2π,

$$\tilde{\Psi}(t_i)=\tilde{\Psi}_i=\Phi_1(t_i)-2\pi i. \tag{13}$$

Wrapping of $\tilde{\Psi}_i$ into the interval $[-\pi;\pi]$ implies $\tilde{\Psi}_i=\Phi_1(t_i)$. That is, by construction, $\tilde{\Psi}_i$ coincides with Ψ_i. Thus, Eq. (8) provides an explicit relation between the angles of return times map and the conventional phase difference up to some constant. This relation will be demonstrated by numerical simulation of a nonstationary process in Van der Pol system in Sec. III B.

A classical sine circle map [42] is usually used to describe the evolution of phase difference $\tilde{\Psi}_i$:

$$\tilde{\Psi}_{i+1}=\tilde{\Psi}_i+\delta+K\sin\tilde{\Psi}_i \pmod{2\pi}, \tag{14}$$

where K is the effective amplitude of external forcing and δ is the frequency detuning between the eigenfrequency of the system and the external forcing. A typical return function of the map (14) is shown in Fig. 5. Let us make a comparison of map (11) with map (14).

The formal difference between Eq. (11) and the sine circle map is the presence of two points at which the distance between the return function and the diagonal is minimal, instead of only one such point. An important distinction is that the map (11), unlike map (14), does not depend on the amplitude of forcing and is thus always one-to-one, so no chaos can be described by it. Another important feature is that the return function of Eq. (14) can cross the diagonal, as parameters K and δ are varied, while in the map (11) it can only touch the diagonal at two points where $\xi=0$ or $\xi=1$, but never crosses it.

It is obvious that, when (i) the approximation of a quasiharmonic oscillator is not valid, and/or (ii) the oscillator is not being forced harmonically, and/or (iii) the amplitude of forcing cannot be considered small, the real map will differ from that predicted theoretically. However, even where one or more of (i)–(iii) apply, but the torus still exists, the qualitative picture remains the same, i.e., for the synchronous regime we will obtain a finite number of points, whereas for the asynchronous one the map will look like a continuous curve.

We have, therefore, arrived at a diagnostic criterion for the existence of synchronization, or the lack of it, between *two* noise-free interacting processes manifested within a one-dimensional signal.

D. Derivation of map for angles for several interacting processes

We now consider the case when a quasiharmonic oscillator is being forced, not just by one, but by n harmonic signals with n independent frequencies Ω_i, $i=1,\ldots,n$. We suppose the amplitude A_i of each of these signals to be much smaller than R. Then, as before, the solution of the resulting nonautonomous system can be approximated by

$$x(t)=R\sin\omega t+\sum_{j=1}^{n}A_j\sin(\Omega_j t+\phi_j^0), \quad A_j\ll R. \tag{15}$$

Here ϕ_j^0 are the initial phase shifts of the solution components. Denote $2\pi\Omega_j/\omega=\Theta_j$. As before, expand Eq. (15) into Taylor series in the vicinity of $t_i^*=2\pi i/\omega$ and neglect all terms beyond the linear ones,

$$x(t)=\sum_{j=1}^{n} A_j \sin(i\Theta_j+\phi_j^0)+\left(t-\frac{2\pi i}{\omega}\right)\times\left(R\omega+\sum_{j=1}^{n} A_j\Omega_j\cos(i\Theta_j+\phi_j^0)\right)=0,$$

to obtain an approximate expression for the moments t_i of the signal's intersection with the zero axis,

$$t_i=-\frac{\sum_{j=1}^{n} A_j \sin(i\Theta_j+\phi_j^0)}{R\omega+\sum_{j=1}^{n} A_j\Omega_j\cos(i\Theta_j+\phi_j^0)}+\frac{2\pi i}{\omega}\approx-\frac{1}{R\omega}\sum_{j=1}^{n} A_j \sin(i\Theta_j+\phi_j^0)+\frac{2\pi i}{\omega}.$$

The return times are defined as

$$T_i=t_{i+1}-t_i=\frac{2\pi}{\omega}-\frac{1}{R\omega}\left[\sum_{j=1}^{n} A_j \sin(i\Theta_j+\phi_j^0+\Theta_j)-\sum_{j=1}^{n} A_j \sin(i\Theta_j+\phi_j^0)\right]=\frac{2\pi}{\omega}-\frac{2}{R\omega}\sum_{j=1}^{n} A_j\cos\left(i\Theta_j+\phi_j^0+\frac{\Theta_j}{2}\right)\sin\frac{\Theta_j}{2}.$$

Then $\tan\phi_i$ is equal to

$$\tan\phi_i=\frac{T_{i+1}-\frac{2\pi}{\omega}}{T_i+\frac{2\pi}{\omega}}=\frac{\sum_{j=1}^{n}\beta_j\cos\left(i\Theta_j+\phi_j^0+\frac{3\Theta_j}{2}\right)}{\sum_{j=1}^{n}\beta_j\cos\left(i\Theta_j+\phi_j^0+\frac{\Theta_j}{2}\right)},$$

where $\beta_j=(A_j/A_1)[\sin(\Theta_j/2)/\sin(\Theta_1/2)]$, $\beta_1=1$. Transform the latter expression to rewrite it in a more convenient form,

$$\tan\phi_i=\left[\sum_{j=1}^{n}\beta_j\cos\left(i\Theta_j+\phi_j^0+\frac{\Theta_j}{2}\right)\cos\Theta_j-\sum_{j=1}^{n}\sin\left(i\Theta_j+\phi_j^0+\frac{\Theta_j}{2}\right)\sin\Theta_j\right]\left[\sum_{j=1}^{n}\beta_j\cos\left(i\Theta_j+\phi_j^0+\frac{\Theta_j}{2}\right)\right]^{-1}. \tag{16}$$

Now add to and subtract from the numerator of Eq. (16) $\cos\Theta_1\,\Sigma_{j=1}^{n}\beta_j\cos(i\Theta_j+\phi_j^0+\Theta_j/2)$, yielding

$$\tan\phi_i=\cos\Theta_1+\left[\sum_{j=2}^{n}\beta_j\cos\left(i\Theta_j+\phi_j^0+\frac{\Theta_j}{2}\right)(\cos\Theta_j-\cos\Theta_1)-\sum_{j=1}^{n}\sin\left(i\Theta_j+\phi_j^0+\frac{\Theta_j}{2}\right)\sin\Theta_j\right]\times\left[\sum_{j=1}^{n}\beta_j\cos\left(i\Theta_j+\phi_j^0+\frac{\Theta_j}{2}\right)\right]^{-1}. \tag{17}$$

By analogy derive the expression for $\cot\phi_{i-1}$, sum it with $\tan\phi_i$, and obtain an expression for ϕ_i,

$$\phi_i=\arctan\left\{2\cos\Theta_1-\cot\phi_{i-1}+2\times\left[\sum_{j=2}^{n}\beta_j\cos\left(i\Theta_j+\phi_j^0+\frac{\Theta_j}{2}\right)(\cos\Theta_j-\cos\Theta_1)\right]\times\left[\sum_{j=1}^{n}\beta_j\cos\left(i\Theta_j+\phi_j^0+\frac{\Theta_j}{2}\right)\right]^{-1}\right\}. \tag{18}$$

Formula (18) is valid for any number of forcing signals of small amplitude applied to the quasiharmonic oscillator [43]. It is important to realize that the validity of this formula is fully justified by the validity of Eq. (15) describing the behavior of the phase variable $x(t)$ of a system forced by several harmonic signals. In Ref. [44] it was shown theoretically that quasiperiodic motion on an m-dimensional torus is structurally unstable for $m\geqslant 3$. This means that, after such a torus is born, an arbitrarily small perturbation of the system can lead to trajectories on its m-dimensional hypersurface becoming Lyapunov unstable. Thus, in principle, even three-frequency quasiperiodic oscillations cannot exist in real systems affected by noise. However, if the perturbation is vanishingly small, then although the trajectories may be unstable, the vector flow remains close to the quasiperiodic one, and formula (18) is valid asymptotically as the perturbation tends to zero.

For forcing by two harmonic signals Eq. (18) takes the form

$$\phi_i=\arctan\left\{2\cos\Theta_1-\cot\phi_{i-1}+2\beta_2[\cos\Theta_2-\cos\Theta_1]\times\left(\beta_2+\frac{\cos\left(i\Theta_1+\phi_1^0+\frac{\Theta_1}{2}\right)}{\cos\left(i\Theta_2+\phi_2^0+\frac{\Theta_2}{2}\right)}\right)^{-1}\right\},$$

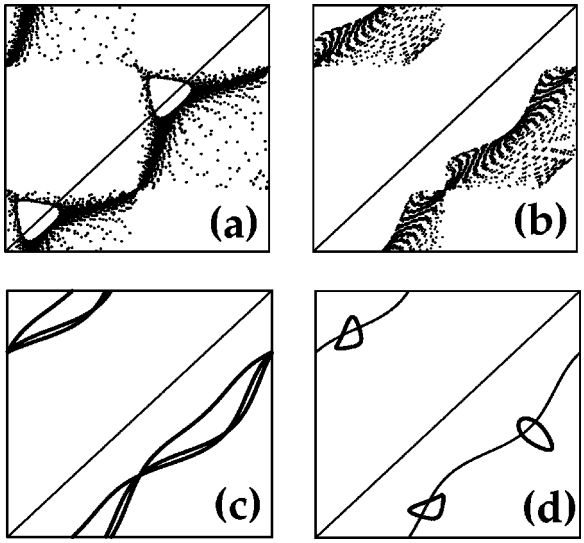

FIG. 6. Phase portraits obtained as the result of iterating map (19) for different parameter values: (a),(b) no synchronization between the three processes involved; (c),(d) partial resonances when only two of three interacting periodic processes are synchronous. Details are given in the text.

$$\beta_2 = \frac{A_2}{A_1} \frac{\sin\frac{\Theta_2}{2}}{\sin\frac{\Theta_1}{2}}. \tag{19}$$

E. Analysis of angles map for three interacting processes

Consider Eq. (19). Note that for more than two interacting processes the resulting map for angles depends on the initial phase shifts ϕ_j^0. First, one can check that, if the second forcing signal is absent, it coincides with Eq. (11). Second, if the frequency of the second forcing signal tends to zero, Eq. (19) also tends to coincide with Eq. (11). Third, if β_2 is not zero, the map (3) is in fact a nonautonomous system, and the forcing represents a nonlinear function of harmonic terms with two independent frequencies, Ω_1 and Ω_2, added to a return function that is similar in form to Eq. (11). Thus, if the map for angles ϕ_i is a one-dimensional curve (or close to it in the presence of noise) one can conclude that only two periodic processes with different time scales are involved in the interaction. But if the map is far from being a one-dimensional curve, this implies that there are at least three interacting processes with different time scales.

Examples of what the phase portrait of the map (19) looks like for four different sets of parameters are shown in Fig. 6. Denote the ''partial'' rotation numbers as ξ_{ij}, where the indices i and j mean the numbers of the processes, and the index 0 signifies the ''basic'' process of frequency ω. Figures 6(a) and 6(b) illustrate the cases where *none* of the three involved periodic processes are synchronized. For (a) $\omega = 1.120\,002\ldots$ (a random sequence of 0, 1, 2, and 3 after the decimal point), $\Omega_1 = 0.2$, $\Omega_2 = 0.111\,011\ldots$ (a random sequence of 0 and 1 after the first ''1''), $A_1 = 0.1$, $A_2 = 0.2$, while for (b) $\omega = 1.012\,002\,3\ldots$ (a random sequence of 0, 1, 2, and 3 after the decimal point), $\Omega_1 = 0.3$, $\Omega_2 = 0.201\,022\ldots$ (a random sequence of 0, 1, 2, and 3 after the first ''2''), $A_1 = A_2 = 0.1$.

Figure 6(c) is an illustration of the case when the two periodic processes with small amplitudes are synchronized, with frequencies: $\Omega_1 = 0.3$, $\Omega_2 = 0.1$ ($A_1 = A_2 = 0.1$), with a corresponding ''partial'' rotation number $\xi_{12} = \frac{1}{3}$, while neither of them is synchronized with the main rhythm with $\omega = 1.0100\ldots$ (a random sequence of 0 and 1 after decimal point). The existence of synchronization between the two processes of small amplitude, and the absence of their synchronization with the main rhythm, is demonstrated by the presence of a fixed number (three in this case) of continuous nonclosed curves in the map.

Figure 6(d) illustrates the case where the other two periodic processes are synchronized, namely, the basic one with $\omega = 1$ and that with $\Omega_1 = 0.\dot{3}$ (where the overdot on the digit indicates a recurring decimal) ($A_1 = 0.1$). The ''partial'' rotation number ξ_{01} is $\frac{1}{3}$. Here, $\Omega_2 = 0.1001\ldots$ (a random sequence of 0 and 1 after the first ''1'') and $A_2 = A_1$. Synchronization with the basic process exhibits itself via the presence of small closed loops in the map for angles. Here, a thin black line marks the return function of the autonomous system (11) for $\xi = \frac{1}{3}$.

In general, for the ideal noiseless case, one can decide immediately, just by inspection of the angles map, which of the three periodic processes are synchronous: the presence of a fixed number of closed loops in the map reflects synchronization of one of the time scales with small amplitude with the ''basic'' rhythm, while the presence of a fixed number of one-dimensional nonclosed curves points to synchronization between the two processes of small amplitude. The case when all three rhythms are synchronous is reflected by a fixed number of points in the map, is thus trivial, and so is not illustrated here.

III. TESTING THE METHOD ON MODELS WITH NOISE

A. Two interacting processes

One of the simplest situations encountered in real (especially living) systems is the interaction of two periodic processes with different time scales. It may, however, be complicated by nonstationarity and by noise. First, consider a *stationary* process in a periodic oscillator with periodic forcing *under the influence of noise*. In Fig. 2(b) the map for angles of return times is shown for the case of effective 1:1 synchronization of Van der Pol system whose stroboscopic section is given in Fig. 2(a). Here, the upper cloud of points on the diagonal corresponds to the smeared stable equilibrium of the stroboscopic map [white point in Fig. 2(a)], and the other points are related to the trace of the unstable manifold. The thin black line plots the return function of map (11) for $\xi = 1$, and the map points fall on it with high accuracy.

Now let us simulate a typical experimental situation when the interacting processes are *nonstationary*, and the nonstationarity exhibits itself in a slow random variation of the eigenfrequency of oscillations. Consider the Van der Pol oscillator (2) with a randomly varying parameter ω, which for

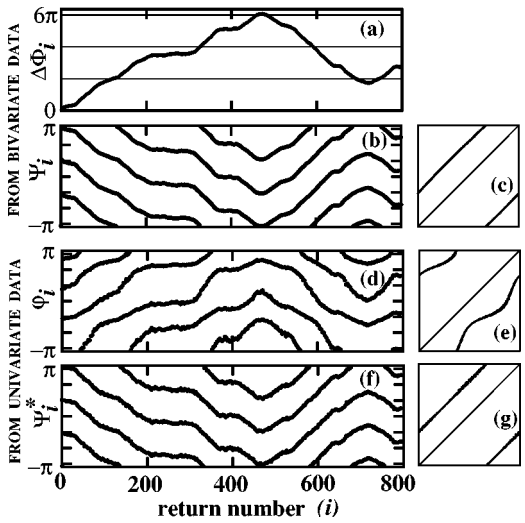

FIG. 7. Comparison of different methods to detect phase synchronization for a forced Van der Pol system with slowly and randomly varying eigenfrequency, Eq. (20). Parameter values are given in the text. The first two rows of plots were derived from *bivariate* data and are (a) the conventional phase difference $\Delta\Phi_i$ between response and forcing; (b) relative phase Ψ_i; (c) map of relative phase Ψ_{i+1} vs Ψ_i. The third and fourth rows are obtained from *univariate* data: (d) angles of return times map; (e) map of angles; (f) angles transformed by means of Eq. (8); (g) map of transformed angles. Note the striking similarity of plots (b) and (f), and (c) and (g), respectively.

small ϵ is approximately equal to the basic frequency of oscillations, under external harmonic forcing:

$$\dot{x}=y,\quad \dot{y}=\epsilon(1-x^2)y-\omega^2 x+C\sin\Omega t,$$

$$\omega=\omega_0+\frac{D_\eta}{\tau}\eta(t),\quad \dot{\eta}=-\frac{\eta}{\tau}+\mu(t), \tag{20}$$

for $\epsilon=0.1$, $\omega_0=1$, $C=0.2$ $\Omega=0.\dot{3}$. $\mu(t)$ is Gaussian white noise $[\langle\mu(t)\rangle=0,\langle\mu(t)^2\rangle=1]$, $\eta(t)$ is colored noise with variance D_η and correlation time $\tau=200$.

The presence or absence of synchronization between self-oscillations and forcing can easily be detected by the conventional method for bivariate data, i.e., by plotting the time dependence of the phase difference between the forcing and the response $\Delta\Phi(t)=\Phi_r(t)-3\Phi_f(t)$, where $\Phi_r(t)$ is the phase of forced oscillations ("response") in the system (20), and $\Phi_f(t)$ is the phase of the external forcing. Consider $\Delta\Phi(t)$ at the moments t_i when the signal $x(t)$ returns to zero in one direction, i.e., when the phase of oscillations changes by 2π. In the absence of noise ($D_\eta=0$) a 1:3 phase synchronization arises, and is detectable through the associated plateau around zero on a $\Delta\Phi(t)$ plot over the whole observation time; the corresponding map (3) consists of three points (this case is trivial and is not illustrated here). For noise variance $D_\eta=0.15$ nonstationary oscillations take place in the system exhibiting epochs of effective 1:3 phase synchronization, which are detectable through the presence of plateaus, and intervals where phase difference slides slowly [Fig. 7(a)].

A phase of forcing at the moments t_i, that is relative phase Ψ_i wrapped into the interval $[-\pi;\pi]$ is shown in Fig. 7(b). The corresponding circle map is shown in Fig. 7(c). Note, that here by construction $\tilde{\Psi}_i=\Psi_i=[\Phi_f(t_i)-2\pi i]\pmod{2\pi}=-\Delta\Phi_i/3\pmod{2\pi}$. In Fig. 7(d) the angles ϕ_i of return times map [45] are shown and their map is given in Fig. 7(e).

Next, we analyze the behavior of the system *using only univariate data*, namely, the variable $x(t)$. From Eq. (8) the relative phase Ψ_i^* is reconstructed from angles ϕ_i whose temporal dependence and map are given in Figs. 7(f) and 7(g), respectively. Note the remarkable correspondence of Figs. 7(b) and 7(f), and 7(c) and 7(g), which clearly demonstrates that the relation (8) still holds even for strongly nonstationary processes. Another significant observation is that maps in Figs. 7(c) and 7(g), being in fact classical circle maps (compare with Fig. 5) are very close to being straight lines, thereby confirming that the forcing was indeed weak.

B. Estimation of rotation number from the angles map

In Ref. [25] a method was suggested to find the rotation number $\xi=n/m$ of synchronization from relative phase Ψ_i: the relative phase is extended to the interval $[0;2\pi n]$, the number n being found by trial; once n is found, the number m is given by the number of horizontal stripes in the plot Ψ_i versus i. The situation becomes complicated if the process is nonstationary and the transition occurs from synchronization with numerator n_1 to that with n_2, where $n_2\neq n_2$, etc. Then one has to find all possible n_i's by trial and error and to estimate all the ξ_i corresponding to each different epoch of synchronization, which can require time and patience.

But we have shown theoretically in Sec. II C for the ideal stationary noiseless case, and confirmed by simulation in Sec. III A for a nonstationary case, that the relative phase Ψ_i can easily be obtained from the angles of return times map, provided that the interaction is weak. Then, in principle, we can apply the already developed technique to the angles and thus estimate the rotation number. However, the angles map has a noticeable advantage over the relative phase, namely, that the shape of a particular angles map is explicitly defined by the value of the rotation number ξ. That means that one can estimate ξ directly from the map without needing to search for the correct value n of the numerator. Equation (10) could be used for the ideal noiseless case, which of course does not arise in reality. In real life situations one can estimate ξ as an average over some temporal window,

$$\langle\xi\rangle=\frac{1}{2\pi}\arccos\frac{s}{2},\quad s=\langle\tan\phi_i+\cot\phi_{i-1}\rangle, \tag{21}$$

where $\langle\cdots\rangle$ implies an average over the window. As one regime gives way to another, the value of $\langle\xi\rangle$ changes, respectively.

The rational rotation number n/m describing synchronization should be close to the one defined by Eq. (21), which we will further refer to as "average rotation number," though not precisely equal to it (due to noise and nonstationarity). It

should be noted that the number of clouds in the angles map does not in general allow one to define the rotation number immediately, because it gives only its denominator m. The same number of clouds m will exist for synchronization with any n, though the clouds will be placed differently. To find the numerator n we suggest finding the approximate rotation number $\langle \xi \rangle$ using formula (21), and then seeking the integer n closest to the value $m\langle \xi \rangle$.

However, before applying formula (21) we should check that it is valid under the circumstances in question, i.e., that the processes under study interact *weakly*. The most straightforward way to check this is to obtain the value of $\langle \xi \rangle$ from Eq. (21), to plot the corresponding return function, and to see if it fits experimental map for angles well enough. If it does, we can accept this $\langle \xi \rangle$ as an approximation of the true rotation number; but if not, we cannot rely on the value in question.

There is also a straightforward way to estimate the rotation number from the angles ϕ_i by using its definition (1). However, to do so one needs to be able to extend the discrete angle ϕ_i in order to make it increase monotonically. In the present paper we use only formula (21) to estimate the rotation number.

The rotation number $\langle \xi \rangle$ for the case of Fig. 7(e) is approximated by formula (21) as 0.333 27...; the number 3 of parallel stripes in Figs. 7(b), 7(d), 7(f) gives the denominator m; and thus the true value of the rotation number corresponding to the epochs of phase locking is $\frac{1}{3}$. The return function of map (11) for $\xi = \frac{1}{3}$ fits the plot in Fig. 7(e) with high accuracy and cannot be distinguished from it, thereby confirming that the interaction is weak.

C. Three interacting processes

The situation where more than two processes with different time scales interact is one that is often encountered in complex living systems. We, therefore, consider the case of three interacting processes in systems affected by weak noise, which we will take to be Gaussian. It is clear that the addition of even weak noise will smear the plots in Fig. 6, affecting our ability to detect synchronization between the different processes. However, the extent of the effect will differ for different rhythms. Namely, closed loops as in Fig. 6(d) are likely to become hard to distinguish from a large number of discrete points; but we will still observe three isolated clouds of points pointing to synchronization between the basic rhythm and the one with smaller amplitude with rotation number $\xi = \frac{1}{3}$. Similarly, the conclusions about the absence of synchronization between the basic rhythm and those with smaller amplitude as illustrated by Fig. 6(c) will remain valid even in the presence of noise.

However, noise will definitely prevent one from making judgments about the fine structure of such plots, thus rendering it almost impossible to establish whether or not the processes with smaller amplitudes are synchronized with each other. Fluctuational smearing of the plot in Fig. 6(c), for example, will prevent one from identifying the number of nonclosed curves (because two of them are likely to merge), and smearing of the plot in Fig. 6(d) will prevent one from distinguishing whether each cloud represents a smeared loop or consists of several smeared points.

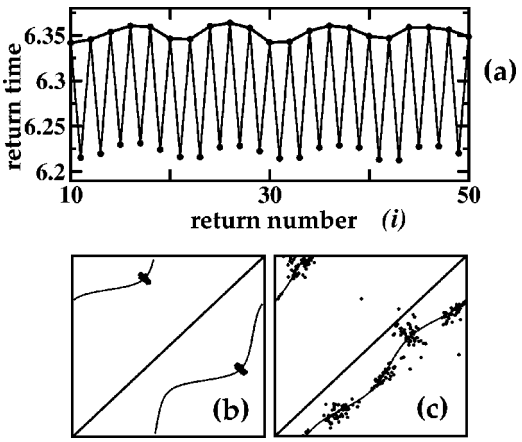

FIG. 8. Quasiperiodically forced Van der Pol system with noise (22). All processes are synchronous. (a) Return times T_i. Local maxima are connected by a thick solid line. (b),(c) Angles-of-return-times map for (b) T_i and (c) local maxima of T_i. Thin black lines show return functions in Eq. (11) for (b) $\xi_{01} = 1/2$ (c) $\xi_{12} = 1/5$.

In view of these problems we suggest an extension of our method to remove from consideration the basic rhythm, thereby enabling us to focus our attention on the smaller amplitude processes. Namely, after detecting synchronization or otherwise between the main rhythm and the one of the remaining two, we propose to proceed as follows. Plot the return times T_i vs i and form a new dataset consisting of all their local maxima (or minima) as shown in Fig. 8(a). Now treat the new data as an independent time series resulting from the interaction of only two processes. One can plot for these data the map of angles and then analyze it by analogy with Sec. III B.

This approach can be realized in application to experimental data only in cases where the frequency of the basic process is larger than those of smaller amplitude. However, this condition is often satisfied in practice, as will be illustrated [46] in relation to human heart rate variability data.

To demonstrate the workability of this technique, we apply it to the Van der Pol system forced quasiperiodically and influenced by noise,

$$\dot{x} = y, \tag{22}$$

$$\dot{y} = \epsilon(1 - x^2)y - \omega_0 x + C_1 \sin \Omega_1 t + C_2 \sin \Omega_2 t + \sqrt{D}\mu(t)$$

for $\epsilon = 0.1$, $\omega_0 = 1$, $C_1 = C_2 = 0.1$, $\Omega_1 = 0.5$, $\Omega_2 = 0.1$, $D = 0.000\,01$. The parameters are selected in such a way that for all the processes effective synchronization takes place, with $\xi_{01} = \frac{1}{2}$ and $\xi_{12} = \frac{1}{5}$. In Fig. 8(a) the sequence of return times T_i extracted from coordinate $y(t)$, and all its local maxima, are shown. In Fig. 8(b) the map for angles is shown for T_i, which consists of two clouds of points (black points) lying on a return function (11) for $\xi = \frac{1}{2}$ (thin black line), being evidence of 1:2 synchronization between the basic pro-

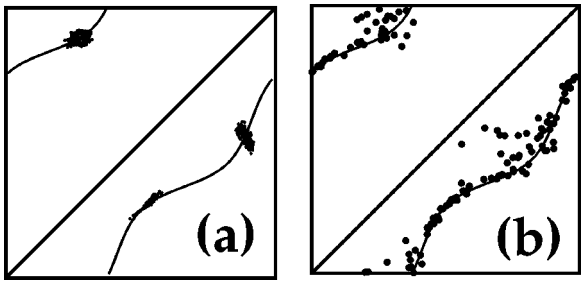

FIG. 9. Quasiperiodically forced Van der Pol system with noise (22). The basic process is synchronous with that with Ω_2. The process with Ω_3 is not synchronous with either of the other two. (a) Angles map for return times map. (b) Angles map for local maxima of return times. The thin black lines show return functions of Eq. (11) for (a) $\xi=1/3$, (b) $\xi=0.3$.

cess and the one with frequency Ω_1. At this stage, it is difficult to decide from looking at the map whether or not the smaller amplitude processes are synchronous. Now, plot the map for angles for the set of local maxima of T_i [Fig. 8(c)]. One can clearly distinguish five separate clouds of points here, pointing to synchronization between the processes with small amplitudes, the denominator m of the rotation number being given by the number of clouds. A rough estimate of the rotation number by Eq. (21) gives 0.212 36 which is close to $\frac{1}{5}$ (the corresponding return function is shown by a thin black line), and so the correct rotation number of $\frac{1}{5}$ has been successfuly extracted.

Now, apply our technique to the case when only partial effective synchronization in Eq. (22) takes place. Set $\epsilon=0.1$, $\omega_0=1$, $C_1=0.3$, $C_2=0.17$, $\Omega_1=0.333\,001$, $\Omega_2=0.1001$, $D=0.0001$. In Fig. 9(a) a map for angles of return times is plotted. Three clouds of points testify to the effective 1:3 synchronization between the basic rhythm and forcing with frequency Ω_1. The ''average rotation number'' calculated from this map by use of Eq. (21) is 0.333 333, which is a very good approximation of $\frac{1}{3}$. With this, the map for angles for local maxima of return times shown in Fig. 9(b) is rather smeared by noise and displays no effective synchronization between forcings. The average rotation number from Eq. (21) is 0.2801 . . . , which is close to the actual frequency ratio of the processes under consideration $\xi_{12}=0.300\,599\ldots$. The return function for the map (11) with parameter $\xi=0.3$, shown by a thin black line, seems to fit the map points reasonably well.

Thus, the technique described above seems to be able to provide information about synchronization, or its absence, between each consecutive (first with second, second with third) pair of three processes interacting within a nonlinear system, even in the presence of noise.

IV. SUMMARY AND DISCUSSION

To summarize, we have proposed an approach to the detection of synchronization (or the lack of it) between two or several processes interacting within a single system, using only a one-dimensional signal coming from it. The approach is based on plotting the map of angles of the return times map, and studying its dynamics. We have revealed an explicit relation between the angles of return times map and the phase difference between interacting processes. The validity of this relation is confirmed also for nonstationary processes in a model.

Explicit maps have been derived describing the behavior of the angles-of-return-times map for a system with a limit cycle forced by an arbitrary number of harmonic signals of small amplitude. The maps obtained appear to describe well numerically simulated data under appropriate conditions.

All the formulas describing the angles' behavior can be derived not only for the return times map, but also for the *stroboscopic* map reconstructed from a one-dimensional signal by the delay method. Moreover, as numerical simulations have shown, they also fit well angles of Poincaré sections reconstructed from one-dimensional time series. The reason for presenting the above discussion in relation to the return times map, rather than for the stroboscopic map, comes back to the reason for writing this paper: to obtain a stroboscopic section we would need to link ourselves to an external forcing, or to a signal from interacting partial subsystem, and these are by definition absent or unknown in the context of the problem posed.

Although the same (or similar) formulas should in principle be obtainable for the reconstructed Poincaré map within the framework of our starting suppositions (4), (15), we failed to do so because of the complicated transcendental equations that arise.

Given a one-dimensional time series, we can find the map for angles by reconstructing either the Poincaré or the return times map. Both of these operations seems equally valid and should lead to the same results for dynamical systems. However, in practice, data from medical or biological experiments are often already presented in the form of return times, like *R-R* intervals of human electrocardiogram. Moreover, the algorithm for extraction of return times can be simpler than that for the Poincaré section, the latter being connected with restoration of the phase portrait in a multidimensional phase space and searching for intersection of the phase trajectory with a secant hypersurface. Of course, one should decide for oneself which method is preferable in any particular case.

V. CONCLUSIONS

Based on the results presented above, we arrive at the following conclusions.

For two weakly interacting processes, the angles of return times map can be transformed to a relative phase by means of Eq. (8).

Without noise, when a weak periodic forcing is applied to a periodic oscillator, the dynamics of angles of return times does not depend on the amplitude of forcing and is completely defined by the rotation number. When a periodic oscillator is forced quasiperiodically and weakly, the dynamics of angles is defined not only by partial rotation numbers, but also by the ratios of the forcing amplitudes.

The technique of eliminating the higher-frequency components by extracting local extrema from the return times allows one to reach a judgment about the synchronization or otherwise of each successive pair of processes involved, for at least three processes.

We, therefore, expect that the proposed approach is likely to be useful in application to the analysis of different kinds of real data, for example, biological. It is applied to heart rate variability data in the paper [46] that follows.

ACKNOWLEDGMENTS

We are much indebted to Dr. Alexander Neiman for valuable discussions and for his constructive comments on a draft version of the manuscript. The work was supported by the Engineering and Physical Sciences Research Council (UK), the Leverhulme Trust, the Medical Research Council (UK), and the U.S. Civilian Research Development Foundation (Award No. REC 006).

[1] B. Van der Pol, Radio Rev. **1**, 704 (1920).
[2] V. I. Arnold, *Complementary Chapters of Ordinary Differential Equation Theory* (Nauka, Moscow, 1978).
[3] A. N. Malakhov, *Fluctuations in Self-Oscillatory Systems* (Nauka, Moscow, 1968) (in Russian).
[4] R. L. Stratonovich, *Topics in Theory of Random Noise* (Gordon and Breach, New York, 1963).
[5] C. Hayashi, *Nonlinear Oscillations in Physical Systems* (McGraw-Hill, New York, 1964); I. I. Blekhman, *Synchronization in Science and Technology* (ASME Press, New York, 1988).
[6] Yo. Kuramoto, Prog. Theor. Phys. Suppl. **79**, 223 (1984).
[7] V. S. Afraimovich, N. N. Verichev, and M. I. Rabinovich, Izv. VUZov, Radiofiz. **29**, 1050 (1989).
[8] L. M. Pecora and T. L. Carroll, Phys. Rev. Lett. **64**, 821 (1990).
[9] V. S. Anishchenko, T. E. Vadivasova, D. E. Postnov, and M. A. Safonova, Radiotekh. Elektron. (Moscow) **36**, 338 (1991); Int. J. Bifurcation Chaos Appl. Sci. Eng. **2**, 633 (1992).
[10] M. Rosenblum, A. Pikovsky and J. Kurths, Phys. Rev. Lett. **76**, 1804 (1996); A. S. Pikovsky, M. G. Rosenblum, G. V. Osipov, and J. Kurths, Physica D **104**, 219 (1997).
[11] A. Neiman, A. Silchenko, V. S. Anishchenko and L. Schimansky-Geier, Phys. Rev. E **58**, 7118 (1998).
[12] A. Neiman, Phys. Rev. E **49**, 3484 (1994).
[13] A. Silchenko, T. Kapitaniak, and V. S. Anishchenko, Phys. Rev. E **59**, 1593 (1999).
[14] B. Shulgin, A. Neiman, and V. Anishchenko, Phys. Rev. Lett. **75**, 4157 (1995).
[15] S. K. Han, T. G. Yim, D. Postnov, and O. Sosnovtseva, Phys. Rev. Lett. **83**, 1771 (1999).
[16] V. S. Anishchenko, A. G. Balanov, N. B. Janson, N. B. Igosheva, and G. V. Bordyugov, Int. J. Bifurcation Chaos Appl. Sci. Eng. **10**, 2339 (2000).
[17] N. F. Rulkov, Chaos **6**, 262 (1996).
[18] P. Tass, M. G. Rosenblum, J. Weule, J. Kurths, A. Pikovsky, J. Volkmann, A. Schnitzler, and H.-J. Freund, Phys. Rev. Lett. **81**, 3291 (1998).
[19] R. C. Elson, A. I. Selverston, R. Huerta, N. F. Rulkov, M. I. Rabinovich, and H. D. I. Abarbanel, Phys. Rev. Lett. **81**, 5692 (1998).
[20] A. Neiman, Xing Pei, D. Russell, W. Wojtenek, L. Wilkens, F. Moss, H. A. Braun, M. T. Huber, and K. Voigt, Phys. Rev. Lett. **82**, 660 (1999).
[21] G. Matsumoto, K. Aihara, Y. Hanyu, N. Takahashi, S. Yoshizava, and J. Nagumo, Phys. Lett. A **123**, 162 (1987).
[22] J. Sturis, C. Knudsen, N. M. O'Meara, J. S. Thomsen, E. Mosekilde, E. Van Cauter, and K. S. Polonsky, Chaos **5**, 193 (1995).
[23] M. Santini, C. Pandozi, F. Colivicchi, F. Ammirati, M. Carmela Scianaro, A. Castro, and F. Lamberti, G. Gentilucci, Eur. Heart J. **21**, 848 (2000); G. Leblanc, C. Michel, P. Y. Laffy, F. Mercier, and J. N. Fabiani, Cardiovasc. Surg. **5**, S8 (1997).
[24] M. Schiek *et al.*, in *Nonlinear Analysis of Physiological Data*, edited by H. Kantz, J. Kurths, and G. Mayer-Kress (Springer, Berlin, 1998).
[25] C. Schäfer, M. G. Rosenblum, J. Kurths, and H.-H. Abel, Nature (London) **392**, 239 (1998).
[26] Milan Palus and Dirk Hoyer, IEEE Eng. Med. Biol. Mag. **17**, 40 (1998).
[27] A. Stefanovska and M. Bračič, Contemp. Phys. **40**, 31 (1999).
[28] A. Stefanovska, H. Haken, P. V. E. McClintock, M. Hožič, F. Bajrović, and S. Ribarič, Phys. Rev. Lett. **85**, 4831 (2000).
[29] H. Bettermann, D. Amponsah, D. Cysarz, and P. Van Leeuwen, Am. J. Physiol. **277**, H1762 (1999).
[30] A. Stefanovska and M. Hožič, Prog. Theor. Phys. Suppl. **139**, 270 (2000).
[31] N. B. Janson, A. G. Balanov, V. S. Anishchenko, and P. V. E. McClintock, Phys. Rev. Lett. **86**, 1749 (2001).
[32] F. Takens, in *Dynamical Systems and Turbulence*, Warwick, 1980, edited by D. A. Rang and L. S. Young, Lecture Notes in Mathematics Vol. 898 (Springer, Berlin, 1981), p. 366.
[33] J. Stark, D. S. Broomhead, M. E. Davies, and J. Huke, Nonlinear Anal., Theory, Methods Appl. **30**, 5303 (1997).
[34] R. Hegger and H. Kantz, Europhys. Lett. **38**, 267 (1997).
[35] N. B. Janson, A. N. Pavlov, A. B. Neiman, and V. S. Anishchenko, Phys. Rev. E **58**, R4 (1998).
[36] H. Herzel, H. Seidel, and H. Warzel, Wiss Z. Humboldt Univ. Berl. [Reihe Medizin] **41**, 51 (1992).
[37] K. Suder, F. R. Drepper, M. Schiek, and H.-H. Abel, Model. Physiol. **44**, H1092 (1998).
[38] J. Godelle and C. Letellier, Phys. Rev. E **62**, 7973 (2000).
[39] The same expressions (10) and (11) can be obtained for the return times map constructed from the time moments when the function $y(t)=\dot{x}(t)$ takes zero values, and also for the stroboscopic section of signal $x(t)$ obtained by delay reconstruction from the values $x_i=x([2\pi/\Omega]i)$ taken over complete periods of the external forcing. For the ideal noiseless case, Eq. (10) provides a direct way of obtaining the rotation number based on the use of only two successive points of the map for angles.

[40] O. E. Rössler, Phys. Lett. **57A**, 397 (1976).
[41] T. E. Vadivasova, A. G. Balanov, O. V. Sosnovtseva, D. E. Postnov, and E. Mosekilde, Phys. Lett. A **253**, 66 (1999).
[42] V. I. Arnol'd, *Geometrical Methods in the Theory of Ordinary Differential Equations* (Springer-Verlag, New York, 1983); J. Guckenheimer and P. Holmes, *Nonlinear Oscillations, Dynamical Systems and Bifurcations of Vector Fields* (Springer-Verlag, New York, 1983); L. Glass, Chaos **1**, 13 (1991).
[43] If two processes are synchronized, but the strength of interaction is large, one cannot use the map (11) to describe the dynamics of angles. However, the resulting signal can still be approximated by a sum of several most significant sine terms with frequencies ω, 2ω,..., Ω, 2Ω,..., $\omega \pm \Omega$, $\omega \pm 2\Omega$,..., etc. Then the map (18) can reliably describe the behavior of angles.
[44] S. Newhouse, D. Ruelle, and F. Takens, Commun. Math. Phys. **64**, 35 (1979).
[45] Since the process is substantially nonstationary, return times oscillate around an average value that is floating randomly. Before extracting angles, this floating average was removed by the technique of derivatives described in Ref. [46].
[46] N. B. Janson, A. G. Balanov, V. S. Anishchenko, and P. V. E. McClintock, following paper, Phys. Rev. E **65**, 036212 (2001).